



Photosynthetic treatment of piggery wastewater in sequential purple phototrophic bacteria and microalgae-bacteria photobioreactors

Cristian A. Sepúlveda-Muñoz^{a,b}, Gorka Hontiyuelo^a, Saúl Blanco^{c,d},
Andrés F. Torres-Franco^{a,b}, Raúl Muñoz^{a,b,*}

^a Institute of Sustainable Processes, Dr. Mergelina, s/n, 47011 Valladolid, Spain

^b Department of Chemical Engineering and Environmental Technology, School of Industrial Engineering, University of Valladolid, Dr. Mergelina, s/n, 47011 Valladolid, Spain

^c Departamento de Biodiversidad y Gestión Ambiental, Facultad de Ciencias Biológicas y Ambientales, Universidad de León, Campus de Vegazana s/n, 24071 León, Spain

^d Laboratorio de diatomología y calidad de aguas, Instituto de Investigación de Medio Ambiente, Recursos Naturales y Biodiversidad, La Serna 58, 24007 León, Spain

ARTICLE INFO

Keywords:

Algae
Nutrient recovery
PPB
Purple non-sulfur bacteria
Swine manure

ABSTRACT

Nowadays, piggery wastewater (PWW) management still represents an unsolved global environmental problem. Photosynthetic processes have emerged as an innovative biological platform capable of performing a cost-effective treatment of wastewater with a concomitant assimilation of nutrients into biomass. In this work, the performance of a purple phototrophic bacteria photobioreactor (PPB-PBR) coupled with a microalgae-bacteria photobioreactor (MB-PBR) was assessed during the treatment of PWW at a hydraulic retention time (HRT) of 12.2 (stage I) and 6.2 days (stages II–VI) and intensities of near-infrared radiation in the PPB-PBR of 30 W m⁻² (stages I–II) and 114 W m⁻² (stages III–IV). Maximum removal efficiencies of total dissolved organic carbon (TOC-RE) and total dissolved nitrogen (TN-RE) of 91% and 82%, respectively, were recorded at an HRT of 12.2 days. The decrease in HRT to 6.2 days reduced the TOC-RE and TN-RE in both photobioreactors, but the increase in near-infrared radiation enhanced TOC-RE in the PPB-PBR, contributing to a global carbon recovery of 67% via assimilation in the form of PPB biomass. PPB-PBR was highly efficient in carbon assimilation, while MB-PBR enhanced nitrogen and total suspended solids removals, with a contribution to TN-RE of 63% and a global decrease in TSS of 76%. The culture broth of PPB-PBR was dominated by *Rhodospirillum rubrum* sp. up to 54%, supported by the high HRT and the increase in near-infrared radiation, while the sequential MB-PBR favoured the dominance of *Mychonastes homosphaera*. This work demonstrated, for the first time, the high efficiency of sequentially coupling PPB and microalgae for the treatment of PWW.

1. Introduction

Piggery wastewater (PWW) is typically characterized by high concentrations of pollutants due to the limited use of water in farms, which hinders its subsequent treatment [1]. This wastewater consists mainly of carbon in the form of volatile fatty acids, and nitrogen in the form of ammonium [2]. Anaerobic digestion has been proposed as the most cost-effective technology for organic matter removal in PWW, but this process is not capable of assimilating the high concentration of ammonia present in this wastewater [3]. On the other hand, activated sludge processes based on denitrification-nitrification are typically implemented during PWW treatment, entailing high operating costs as a result of the intensive aeration needed and a detrimental waste of nutrients. In

this context, photosynthetic processes have been recently proposed as a cost-effective platform for carbon and nutrient recovery from PWW [2,4–6].

Photosynthetic microorganisms are one of the life precursors on Earth. These microorganisms can perform photosynthesis using the energy from the solar electromagnetic spectrum, absorbing and transforming solar radiation into chemical energy in the form of biomass [7]. Purple phototrophic bacteria (PPB) are a versatile group of photosynthetic microorganisms capable of growing chemotrophically or phototrophically [8,9]. PPB can absorb the near-infrared electromagnetic spectrum (800 and 1100 nm) due to the presence of bacteriochlorophylls pigments [10,11], exhibiting an advantage to power their metabolism and a unique spectral niche. PPB also contain carotenoids

* Corresponding author at: Institute of Sustainable Processes, Dr. Mergelina, s/n, 47011 Valladolid, Spain.

E-mail address: mutora@iq.uva.es (R. Muñoz).

<https://doi.org/10.1016/j.jwpe.2022.102825>

Received 17 February 2022; Received in revised form 2 April 2022; Accepted 24 April 2022

Available online 3 May 2022

2214-7144/© 2022 The Authors. Published by Elsevier Ltd. This is an open access article under the CC BY license (<http://creativecommons.org/licenses/by/4.0/>).

pigments that confer them their characteristic orange to purple colour [10,12]. On the other hand, microalgae represent the most studied group of photosynthetic microorganisms in recent years as a result of the worldwide interest in microalgae biodiesel and CO₂ capture. Green microalgae, cyanobacteria and diatoms can absorb the visible part of the solar spectrum (400–700 nm) due to the presence of carotenoids and chlorophylls pigments [11].

In this context, PPB have emerged as an alternative biological platform to PWW treatment as a result of their high carbon assimilation [4,6] but with limited nitrogen removal capacity [6,13]. In addition, PPB can grow at low temperatures of about 10–11 °C [14,15], are tolerant to high salinity [16] and to the pollutants present in most types of wastewaters, being able to assimilate all forms of nitrogen [17], and exhibit high growth rates under photoheterotrophic conditions [8]. On the other hand, the use of microalgae-based photobioreactors for the treatment of PWW has been consistently reported in recent years [2], but high PWW dilutions were often needed to prevent microalgae inhibition by NH₃, despite their high nitrogen removal capacity [4,6]. The potential of PPB and microalgae for PWW treatment has been systematically assessed separately in previous studies [4,5], revealing the high carbon assimilation and rapid growth of PPB, and the high nitrogen removal capacity of microalgae. However, the use of PPB as a pre-treatment for microalgae-based PWW treatment has not been yet investigated.

In this work, the potential of an innovative photobioreactor configuration composed of a PPB enclosed anaerobic photobioreactor coupled to sequential microalgae-bacteria open aerobic photobioreactor for the treatment of PWW was systematically investigated, for the first time, under continuous mode during long term operation. The effect of the hydraulic retention time (HRT) and near-infrared radiation on the removal efficiency and assimilation potential of carbon and nitrogen from PWW was assessed through mass balances and a complete characterization of the bacterial and microalgae communities in the photobioreactors was also carried out.

2. Materials and methods

2.1. Inocula and piggery wastewater

The inoculum of the PPB photobioreactor (PPB-PBR) was enriched from a previous culture treating PWW under batch conditions [18]. Fresh PPB inoculum was prepared in 1.2 L gas-tight bottles (Afora, Spain) with helium in the headspace and incubated under magnetic agitation at 300 rpm, 30 °C and near-infrared (NIR) radiation at 50 W m⁻². The inoculum of the microalgae-bacteria photobioreactor (MB-PBR) was taken from an outdoors pilot-scale microalgae photobioreactor treating digestate and biogas [19]. Before inoculation, the PPB and microalgae-bacteria consortia were centrifuged at 10000 rpm for 10 min in a Sorvall Legend RT centrifuge (ThermoScientific, Germany) and resuspended in fresh PWW. PWW was obtained from a nearby pig farming in Segovia (Spain) and maintained at 4 °C. PWW was initially centrifuged on-site in an industrial decanter and diluted 10 folds in tap water, which resulted in constant pH of 7.6 ± 0.1 and average dissolved concentrations of total organic carbon (TOC) of 0.863 ± 0.064 g L⁻¹, total carbon (TC) of 0.974 ± 0.067 g L⁻¹, inorganic carbon (IC) of 0.109 ± 0.022 g L⁻¹, total nitrogen (TN) of 0.341 ± 0.042 g L⁻¹, NH₄⁺ of 0.260 ± 0.080 g L⁻¹ and total suspended solids (TSS) of 0.571 ± 0.065 g L⁻¹.

2.2. Experimental set-up

The configuration of photobioreactors herein assessed consisted of two interconnected photobioreactors of 3 L of working volume (0.2 m length × 0.1 m width × 0.15 m depth) made of PVC. The PPB-PBR was hermetically sealed with a transparent methacrylate lid to promote photo-anaerobic conditions, while the MB-PBR was opened to the

atmosphere to mimic a high rate microalgal pond (Fig. 1). Both photobioreactors were interconnected to 1 L conical settlers. The photobioreactors were agitated with two centrifugal external pumps (EHEIM, Germany) to prevent the heating of the cultivation broth caused by submerged pumps [18]. The PPB-PBR was illuminated with a near-infrared LED panel (centroid emitting at 810 and 850 nm) at 30 W m⁻² (stages I–II) and 114 W m⁻² (stages III–IV). The MB-PBR was illuminated with a white light LED panel at photosynthetic active radiations (PAR) of 1106 μmol m⁻² s⁻¹ (Fig. S1). Both photobioreactors were illuminated with light:dark cycles of 12:12 h. The headspace of the PPB-PBR was flushed with a gas stream of 70% N₂ and 30% CO₂ (Abello Linde, Spain) at 8.7 L d⁻¹ during the light phase. Both photobioreactors were initially operated at an HRT of 12.2 days using 10 folds diluted PWW (stage I, 81 days). The HRT was decreased to 6.2 days using the same PWW dilution (stage II, 73 days). In stage III (46 days), the NIR radiation in the PPB-PBR was increased from 30 to 114 W m⁻². The MB-PBR was reinoculated by day 203 with fresh microalgae-bacteria biomass from an outdoors pilot-scale microalgae-bacteria photobioreactor treating food waste digestate and operated for 63 days, until the end of stage IV. Each settler was purged daily with a volume of 75 mL (stage I), 150 mL (stages II and III, stage IV in PPB-PBR) and 100 mL (stage IV in MB-PBR).

Samples from the influent PWW (40 mL), cultivation broth (20 mL), settled biomass (20 mL) and effluent (40 mL) were systematically drawn twice a week to monitor pH (Fig. S2A), dissolved oxygen (Fig. S2B), temperature (Fig. S2C), culture absorbance (Fig. S3) and TOC, TC, IC, TN (dissolved and total), NH₄⁺ and TSS concentrations. In addition, gas samples from the inflow and outflow of the PPB-PBR were taken to monitor the concentrations of CO₂, CH₄ and H₂S. A sample of the settler of each photobioreactor was drawn, centrifuged (10,000 rpm for 10 min at 4 °C) and dried to analyze the elemental composition (C, H, O, N and S) of the settled biomass. Finally, a sample of the cultivation broth of each photobioreactor under steady-state was stored at –20 °C and 4 °C (with lugol acid and formaldehyde) for 16S ribosomal RNA gene (16S rRNA) sequencing and microalgae taxonomy analysis, respectively.

The steady-state removal efficiencies (REs) of total organic carbon, total nitrogen and TSS were calculated according to García et al. [4] considering the evaporation rates (Eqs. (S1)–(3)). Carbon and nitrogen transformations were assessed based on recovery mass balance (Eqs. (S4)–(33)), under the assumption that carbon losses were associated with CO₂ volatilization or with biofilm formation, whereas nitrogen losses corresponded to N₂ or NH₃ volatilization by denitrification or stripping, respectively [20]. In addition, the carbon and nitrogen assimilated in the form of biomass were regarded as the sum of the carbon or nitrogen present in the biomass wasted daily from the bottom of the settlers and the biomass present as suspended solids in the liquid effluent from the settlers.

2.3. Analytical methods

The monitoring of temperature and dissolved oxygen concentrations in the photobioreactor cultivation broths was conducted with a Profi-Line 3320 m coupled with a sensor CelloX 325 (WTW, Germany). pH measurements were carried out with a pH 510 pH meter (Cyberscan, The Netherlands). NIR radiation was measured with a PASPort PS-2148 (PASCO, USA), while PAR was measured with a LI-250A light meter (LI-COR Biosciences, Germany). The dissolved and total TOC, TC, IC and TN concentrations were determined in a TOC-VCSH/TN analyzer (Shimadzu, Japan). Culture absorbance measurements were carried out in a UV-2550 spectrophotometer (Shimadzu, Japan) with a spectral scanning between 350 and 850 nm. TSS concentration was determined according to Standard Methods [21]. NH₄⁺ concentration was analyzed with an Orion Dual Start sensor (ThermoScientific, The Netherlands). The elemental composition of the dried biomass (previously washed) was measured in an elemental composition analyzer EA Flash 2000 coupled with a TCD detector (ThermoScientific, The Netherlands). Gas

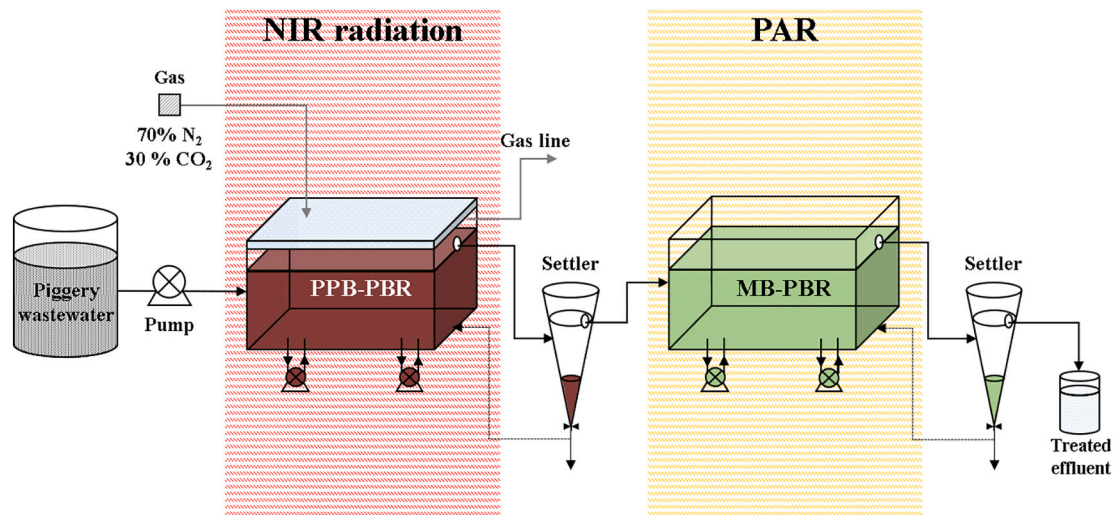


Fig. 1. Schematic diagram of the combined PPB-PBR and MB-PBR used for PWW treatment. The system was composed of a PWW tank, an enclosed photobioreactor with PPB (PPB-PBR) and its corresponding settler interconnected to an open microalgae-bacteria photobioreactor (MB-PBR) with its corresponding settler, discharging into an effluent tank.

concentration was determined in a gas chromatograph 430 GC-TCD (Bruker, USA) according to Ángeles et al. [22].

2.4. DNA sequencing and metagenomic analysis

Genomic DNA was extracted with FastDNA SPIN Kit (MP Biomedical, USA) according to the manufacturer's instructions. The amplification of 16S rRNA gene was conducted with oligonucleotide specific of V3 (5'-TCGTCGGCAGCGTCAGATGTGTATAAGAGA-CAGCCTACGGGNGGCWGCAG-3') and V4 (5'-GTCTCGTGGGCTCGGAGATGTGTATAAGAGACAGGACTACHVGGGTATCTAATCC-3') regions. The libraries were sequenced using a MiSeq Sequencer (Illumina, USA) according to the manufacturer's instructions. Sequencing and bioinformatic analyses were carried out by the foundation for the promotion of health and biomedical research of Valencia region (Spain). Quality assessment was performed using the PRINSEQ-lite program [23]. Paired-ends joining, chimera and denoising depletion were performed starting from paired ends data using the open-source software DADA2 pipeline [24]. The SILVA database was used for taxonomic assignment [25]. Taxonomic affiliations have been assigned using the Naive Bayesian classifier using the open-source software QIIME 2 [26].

2.5. Taxonomic identification of microalgae

Samples of 1.5 mL of the MB-PBR cultivation broth under steady-state were fixed with 5% of lugol acid and 10% of formaldehyde. The microalgae population was counted and identified using an inverted microscope IX70 (OLYMPUS, USA) according to a phytoplankton manual [27].

2.6. Statistical methods

The experimental data was always obtained under steady-state, exhibiting normal distribution (Shapiro-Wilk test). Statistical analyses were performed with the software Statgraphics Centurion version 18. An ANOVA analysis of variance was conducted to determine the significance of the values obtained by performing a Tukey test with a value of $p < 0.05$ considered significant.

3. Results and discussion

3.1. Piggery wastewater treatment performance

3.1.1. Environmental parameters

Microbial activity in both PPB-PBR and MB-PBR was favoured by the constant average temperatures of 25 °C over the entire experimental period (Table 1 and Fig. S2C). The overheating of the cultivation broth was prevented by the implementation of external recirculation pumps. Compared to PWW, more neutral conditions at an average pH of 6.9 ± 0.2 were recorded in PPB-PBR, due to the blanketing of PPB-PBR headspace with CO₂ and to the effective consumption of organic acids by PPB [10]. On the other hand, the enclosed configuration of this photobioreactor avoided any oxygen transfer from the atmosphere to the cultivation broth, thus maintaining anaerobic conditions at low dissolved oxygen concentrations of 0.03 ± 0.01 mg O₂ L⁻¹ (Fig. S2B), and preventing water evaporative losses during the four operational stages. Although PPB are capable of growing under aerobic or anaerobic conditions, with chemotrophic or phototrophic metabolisms, respectively [9], anaerobic conditions likely favoured PPB growth more than that of any other chemotrophic bacteria [8,18].

In MB-PBR, the average pH of 8.1 ± 0.2 entailed the occurrence of more alkaline conditions than in PWW and PPB-PBR, as a consequence of the photosynthetic CO₂ consumption by microalgae (Table 1 and Fig. S2A). In addition, the prevailing low dissolved oxygen concentrations of 0.06 ± 0.03 mg O₂ L⁻¹ in MB-PBR during the entire experiment suggested that microalgae photosynthetic oxygenation supported only partial oxidation of the organic matter and NH₄⁺ by aerobic bacteria [20,28], which utilized the oxygen as an electron donor [4]. Conversely, the open configuration of the MB-PBR resulted in higher evaporative losses compared to PPB-PBR, which averaged 44%, 38%, 36% and 30% in stages I, II, III and IV, respectively (Table 1).

3.1.2. Carbon fate

TOC concentrations in PWW remained constant during all operational stages at 0.863 ± 0.064 g L⁻¹ (Table 1, Fig. 2A). During stage I, PPB-PBR supported a steady-state removal of dissolved TOC of $67 \pm 3\%$, resulting in a final effluent concentration of 0.277 ± 0.038 g TOC L⁻¹. A similar trend was recorded for the total TOC, which was removed with an efficiency of $52 \pm 4\%$, resulting in an effluent total TOC concentration of 0.489 ± 0.029 g L⁻¹ (Fig. 2B). These TOC removals were the highest recorded as a result of the high HRT and photo-anaerobic

Table 1

Summary of the main physical-chemical parameters of the PWW (10 fold diluted in tap water), cultivation broth and effluent of the PPB-PBR and MB-PBR during steady-state under the different operational stages.

| Parameters | PWW | Stage I | | Stage II | | Stage III | | Stage IV | |
|---|-------------|-------------|-------------|-------------|-------------|-------------|-------------|-------------|-------------|
| | | PPB-PBR | MB-PBR | PPB-PBR | MB-PBR | PPB-PBR | MB-PBR | PPB-PBR | MB-PBR |
| Temperature (°C) | – | 26.3 ± 2.2 | 25.6 ± 2.2 | 23.1 ± 2.1 | 23.1 ± 1.8 | 25.0 ± 2.0 | 24.0 ± 1.7 | 26.6 ± 2.2 | 24.9 ± 1.8 |
| pH | 7.6 ± 0.1 | 6.9 ± 0.2 | 8.2 ± 0.2 | 6.8 ± 0.1 | 8.2 ± 0.1 | 6.9 ± 0.1 | 8.0 ± 0.1 | 7.1 ± 0.2 | 8.1 ± 0.1 |
| NIR radiation (W m ⁻²) | – | 28.4 ± 2.3 | – | 30.0 ± 2.1 | – | 113.6 ± 2.2 | – | 113.7 ± 3.3 | – |
| PAR (μmol m ⁻² s ⁻¹) | – | – | 1093 ± 46 | – | 1100 ± 24 | – | 1122 ± 16 | – | 1122 ± 13 |
| Evaporation (%) | – | – | 44 ± 5 | – | 38 ± 7 | – | 36 ± 7 | – | 30 ± 7 |
| TOC (g L ⁻¹) | 0.86 ± 0.06 | 0.28 ± 0.04 | 0.14 ± 0.01 | 0.33 ± 0.05 | 0.17 ± 0.02 | 0.22 ± 0.03 | 0.14 ± 0.01 | 0.24 ± 0.02 | 0.16 ± 0.01 |
| TN (g L ⁻¹) | 0.34 ± 0.04 | 0.26 ± 0.02 | 0.10 ± 0.01 | 0.33 ± 0.01 | 0.24 ± 0.02 | 0.27 ± 0.02 | 0.20 ± 0.02 | 0.28 ± 0.01 | 0.19 ± 0.02 |
| NH ₄ ⁺ (g L ⁻¹) | 0.26 ± 0.08 | 0.23 ± 0.04 | 0.05 ± 0.02 | 0.18 ± 0.06 | 0.08 ± 0.02 | 0.18 ± 0.04 | 0.12 ± 0.02 | 0.14 ± 0.04 | 0.09 ± 0.02 |
| TSS (g L ⁻¹) | 0.57 ± 0.07 | 0.92 ± 0.10 | 1.66 ± 0.24 | 0.67 ± 0.06 | 1.42 ± 0.20 | 0.71 ± 0.06 | 1.28 ± 0.13 | 0.59 ± 0.10 | 1.35 ± 0.13 |
| TSS effluent (g L ⁻¹) | – | 0.75 ± 0.09 | 0.25 ± 0.14 | 0.64 ± 0.04 | 0.47 ± 0.04 | 0.60 ± 0.08 | 0.31 ± 0.07 | 0.47 ± 0.08 | 0.26 ± 0.10 |

(–) Not applicable. (±) Values represent average ± standard deviation (n = 7) obtained under steady-state.

TOC, TN and NH₄⁺ correspond to the dissolved concentration in the effluent of each photobioreactor.

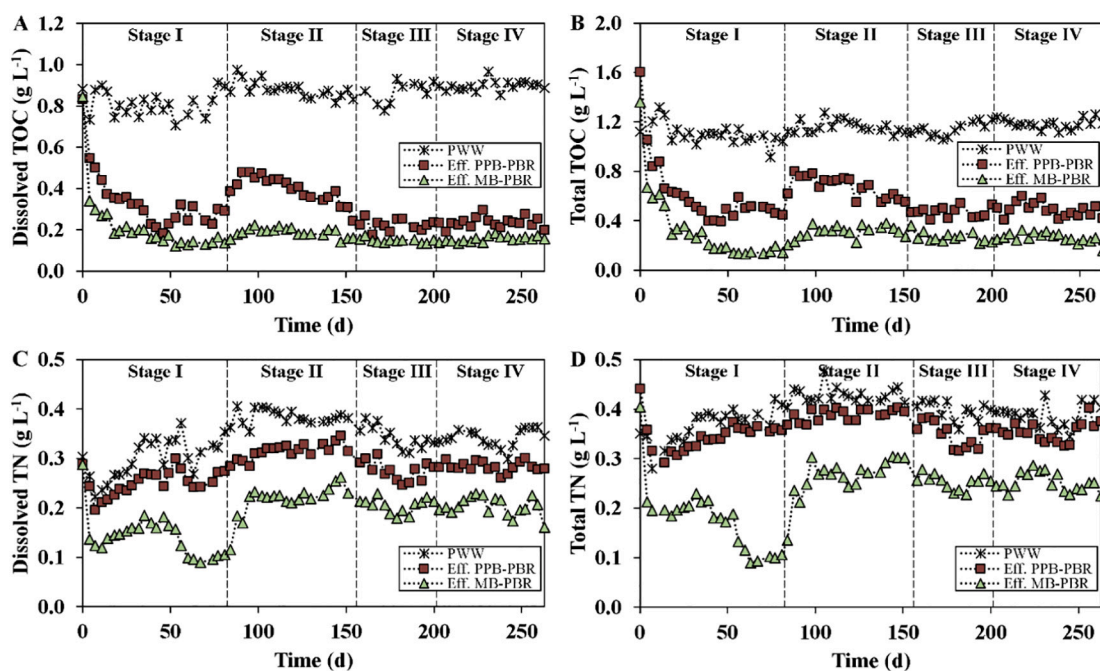


Fig. 2. Time course of the concentration of dissolved TOC (A), total TOC (B), dissolved TN (C) and total TN (D) in the PWW, effluent from the PPB-PBR and effluent from the MB-PBR.

conditions promoting effective assimilation of carbon by the photoheterotrophic metabolism of PPB. Similar studies have recently reported high carbon removals by PPB under photo-anaerobic conditions [8]. In this context, multiple metabolic pathways in PPB likely contributed to the high removal of carbon recorded in PPB-PBR, more specifically: the pentose phosphate pathway, Embden-Meyerhof pathway, tricarboxylic acid (TCA) cycle and even the Calvin-Benson-Bassham pathway, all encoded in *Rhodospseudomonas palustris* genome [9]. These last two metabolic pathways may have played a major role in carbon assimilation in PPB-PBR, contributing to the assimilation of volatile fatty acids in the form of PPB biomass via TCA [13,29] or by fixing the CO₂ metabolically produced [30]. Nevertheless, CO₂ assimilation seemed to be negligible since the CO₂ supplied to PPB-PBR, estimated as the difference between the inlet and outlet mass flowrate of CO₂ (average value of 0.209 g d⁻¹) (Fig. S4A), increased the IC concentration of the cultivation broth during stage I from 0.099 ± 0.010 to 0.236 ± 0.017 g L⁻¹. Indeed, the external addition of CO₂ was mainly performed to maintain a neutral pH and to avoid the inhibition of PPB metabolism [13]. Neither H₂S nor CH₄ were detected in the headspace of PPB-PBR during stage I (Fig. S4B and S4C).

On the other hand, during stage I, MB-PBR supported lower removal of dissolved TOC (23 ± 3%) and total TOC (40 ± 5%) compared to PPB-PBR, which resulted in dissolved TOC concentrations ranging from 0.277 ± 0.038 g L⁻¹ to 0.173 ± 0.022 g L⁻¹ in the final effluent (Fig. 2A). The high efficiency of microalgae-bacteria symbiotic consortia in removing carbon from wastewater has been previously demonstrated in several studies [20,22,31]. Herein, higher removals in the microalgal-bacterial pond were restricted mainly by the limited photosynthetic oxygenation in the process, which ultimately limited aerobic bacterial activity. The consumption of the most readily biodegradable organic matter in PPB-PBR also resulted in lower TOC removals in MB-PBR. Furthermore, the low IC removal by microalgae also evidenced the limited autotrophic activity in MB-PBR despite previous studies have shown the great potential of microalgae for carbon assimilation during PWW treatment [2,4,32]. The relatively low concentrations of microalgae below (<10⁹ cell L⁻¹) were probably the main constrain in the performance of MB-PBR [33]. Nevertheless, microalgae showed the highest activity during stage I, as evidenced by the highest culture absorbance at 680 nm (used as an indicator of the presence of chlorophyll *a*) compared to the following operational stages (Fig. S3). The long

HRT of 12 days likely enhanced the growth of microalgae in PWW [28]. Overall, the combination of PPB-PBR and MB-PBR supported a final effluent TOC concentration of $0.140 \pm 0.012 \text{ g L}^{-1}$, corresponding to a global TOC-RE of $92 \pm 1\%$ during stage I. This TOC-RE was the highest recorded, likely fostered by the high HRT promoting high assimilation of carbon via photoheterotrophic PPB growth in PPB-PBR and microalgae-bacteria symbiosis in MB-PBR.

During stage II, the decrease in HRT from 12.2 to 6.2 days significantly lowered the dissolved and total TOC-RE to $61 \pm 4\%$ and $49 \pm 6\%$ (Fig. 3A) in PPB-PBR, respectively, which were relatively high based on the fact that PPB-PBR operated at 3.1 days. Similar to stage I, carbon assimilation by PPB contributed to the high removals recorded. Interestingly, from day 112 onwards, a fraction of the TOC removed (4%) was transformed into CH_4 , resulting in a steady-state concentration in the outflow gas of the PPB-PBR of $15 \pm 1 \text{ g m}^{-3}$ (Fig. S4C). The production of CH_4 was likely related to the higher organic load in the PPB-PBR as a result of the lower HRT, which ultimately favoured the steady entrance of methanogenic archaea from pig faeces [34] into PPB-PBR. The production of H_2S was not detected during the entire experiment (Fig. S4B). On the other hand, the total TOC-RE of MB-PBR of $28 \pm 7\%$ resulted in a global TOC-RE of $77 \pm 2\%$ and a final TOC effluent concentration of $0.173 \pm 0.022 \text{ g L}^{-1}$ during stage II (Fig. 2A). The lower TOC-RE in MB-PBR compared to stage I was likely mediated by the decrease in HRT. In

this context, a comparative study of PPB and microalgae in separate photobioreactors treating PWW reported that a decrease of the HRT from 10.6 to 4.1 resulted in a gradual deterioration of carbon removal efficiency in both PPB (from 84 to 66%) and microalgae (from 87 to 77%) photobioreactors [4].

The increase in NIR radiation in PPB-PBR during stages III and IV resulted in higher dissolved TOC-RE ($75.0 \pm 2.5\%$ and $73.8 \pm 1.9\%$, respectively) and total TOC-RE ($60 \pm 4\%$ and $61 \pm 2\%$, respectively) compared to stage II. The increase in NIR radiation from 30 to 114 W m^{-2} favoured the anoxygenic photosynthesis of PPB, allowing higher assimilations of TOC in PPB-PBR. NIR radiation, which contains less energy compared to visible radiation, facilitates the specific selection of PPB [10]. Although PPB have been reported as capable of treating domestic wastewater at lower intensities of NIR radiation (1.4 and 3 W m^{-2}) [35], PWW contains higher solids concentrations compared to domestic wastewater, thus supporting a higher limitation to light penetration. In this context, a simple comparison with the intensity of solar irradiance on a clear day, which is approximately $\approx 1000 \text{ W m}^{-2}$ and contains 54% in the near-infrared range [36,37], suggests that a PPB-PBR exposed to direct sunlight would receive sufficient NIR radiation to treat PWW. A similar experiment has recently demonstrated the feasibility of PWW treatment under direct solar radiation using UV-VIS absorbing foil for retaining over 90% of ultraviolet and visible radiation [38]. In addition, similar to stage II, a small fraction of TOC (7%) was transformed to CH_4 during stages III and IV, resulting in CH_4 concentrations of $26 \pm 3 \text{ g m}^{-3}$ and $24 \pm 2 \text{ g m}^{-3}$, respectively, in the outflow gas.

In MB-PBR, a lower steady-state dissolved TOC-RE of $12 \pm 3\%$ and total TOC-RE of $23 \pm 5\%$ were achieved during stage III, which was mainly attributed to the highly efficient assimilation of readily biodegradable TOC in PPB-PBR under higher NIR radiation. Conversely, the low HRT during stage III resulted in microalgae wash-out in MB-PBR, which was evidenced by the loss of the characteristic green colour of microalgal photobioreactors [28]. This microalgae loss was also evidenced by the lower absorbance at 680 nm and TSS concentrations by the end of stage III compared to previous stages. The reinoculation of MB-PBR by day 203 increased the presence of microalgae in the culture broth, as indicated by the increase in culture absorbance at 680 nm (Fig. S3), allowing to maintain a total TOC-RE of $23 \pm 2\%$, similar to the efficiency recorded in stage III. The global TOC-RE and TOC concentration in the final effluent accounted for $83 \pm 3\%$ and $84 \pm 2\%$, and 0.145 ± 0.008 and $0.160 \pm 0.007 \text{ g L}^{-1}$ during stages III and IV, respectively. Similarly, the removal of dissolved TOC in the combined PPB-PBR and MB-PBR averaged $87.3 \pm 1.0\%$ and $85.5 \pm 0.6\%$, respectively.

The results obtained confirmed the efficient removals of organic carbon from PWW by PPB and microalgae reported in the literature [4]. The carbon mass balances (Eqs. (S4) and (S19)) revealed that total assimilation into PPB biomass accounted for 20, 21, 20 and 15% of the total input of carbon during stages I, II, III and IV, respectively, standing out as the main removal mechanism during all stages (Table S1), excepting stage IV where a higher share of carbon was stripped from the culture broth. A fraction of the input carbon ranging from 9 to 13% remained as carbon assimilated but lost as suspended solids in the effluent due to the poor settleability of PPB cells. Unassimilated carbon in the liquid effluent of PPB-PBR accounted for 13–22%, whereas the shares of carbon loss of 18, 16, 18 and 30% were recorded during stages I, II, III, IV, respectively, likely due to its retention in biofilms growing attached to the walls of the photobioreactor or CO_2 stripping during the dark idle phase in PPB-PBR. On the other hand, the microalgal-bacterial symbiosis in MB-PBR enhanced carbon assimilation, which represented total shares of 53, 48, 41 and 38% of the carbon input during stages I, II, III and IV, respectively (Table S2). Average carbon values of 12–33% remained unassimilated in the effluent, while 27 to 35% of the carbon input was stripped-out from the photobioreactor cultivation broth.

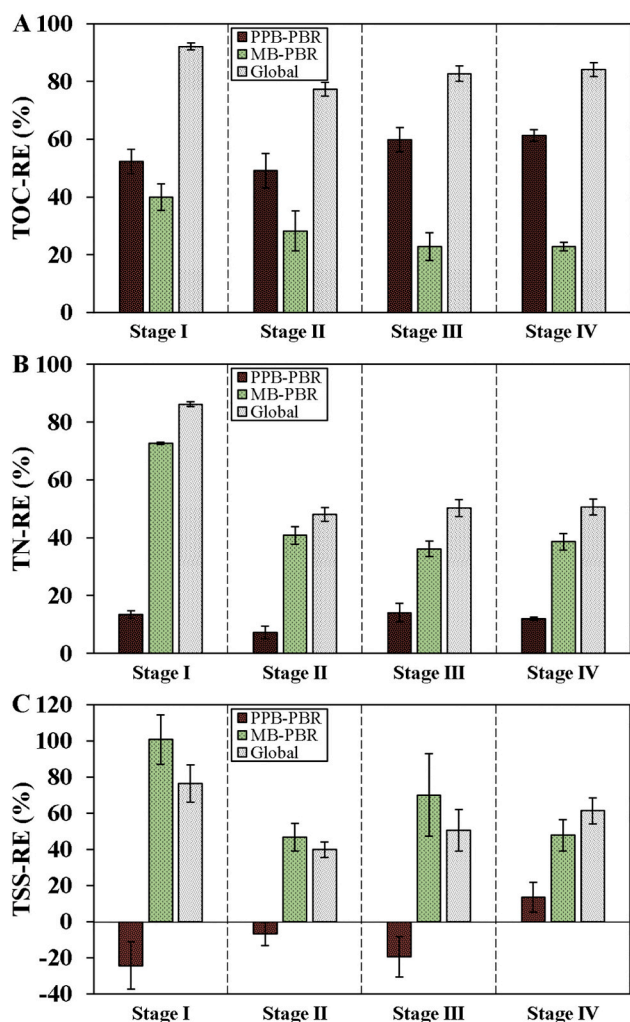


Fig. 3. Steady-state removal efficiencies of TOC (A), TN (B) and TSS (C) in the PPB-PBR, MB-PBR and combined system along the different operational stages. Removal efficiencies were estimated considering the evaporation rate in the photobioreactors.

3.1.3. Nitrogen fate

PWW is typically characterized by high TN and NH_4^+ concentrations. NH_4^+ was the main nitrogen species in the PWW, with a share of 76% of the TN. During stage I, PPB-PBR exhibited low removals of TN ($13 \pm 1\%$) (Fig. 3B) and dissolved TN ($19 \pm 6\%$), likely limited by the lack of biodegradable carbon for nitrogen assimilation into PPB biomass. Thus, previous studies where acetate or ethanol was supplemented as an external carbon source to increase the C:N ratio reported higher nitrogen removals [10,38,39]. Nevertheless, similar TN removals of 13–19% have been previously reported using PPB for the treatment of PWW or domestic wastewater without additional carbon supplementation [5,6]. Interestingly, high nitrogen removals (TN-RE of $73 \pm 0\%$) were supported in MB-PBR, entailing a global TN-RE of $86 \pm 1\%$ in stage I. This was the highest value achieved in the experiment and resulted in an effluent with a low dissolved TN concentration of $0.098 \pm 0.006 \text{ g L}^{-1}$ (Fig. 2C) and a similar trend was recorded for the total TN concentration over the entire experimentation (Fig. 2D). The high affinity of microalgae for NH_4^+ as a nitrogen source [28,40] and their remarkable ability to synthesize amino acids (aspartate, glutamate and glutamine) and proteins [40] at a high content, along with bacterial nitrification-denitrification, mediated the high TN removals recorded in the MB-PBR [4,32].

In stage II, the decrease in HRT to 6.2 days negatively impacted the assimilation of nitrogen, resulting in average steady-state TN-REs of $7 \pm 2\%$ and $41 \pm 3\%$ in PPB-PBR and MB-PBR, respectively. These removals entailed global efficiencies of $48 \pm 2\%$ and $52 \pm 3\%$, for total and dissolved TN, respectively. This decrease in HRT likely resulted in relatively lower nitrogen assimilation by PPB and microalgae due to the higher nitrogen loading rates at 6.2 days compared to 12.2 days.

During stages III and IV, the increase in NIR radiation (114 W m^{-2}) impinging into the PPB-PBR contributed to overcoming the limitations derived from the operation at low HRTs, likely enhancing anoxygenic photosynthesis and protein synthesis, and fostering higher TN-REs of $14 \pm 3\%$ and $12 \pm 1\%$, respectively, which were similar to the efficiencies observed in stage I. On the other hand, MB-PBR achieved an average TN-RE of $36 \pm 3\%$ during stage III, only slightly lower than in stage II but sufficient to maintain a high global TN-RE of $50 \pm 3\%$. During stage IV, MB-PBR supported a TN-RE of $39 \pm 3\%$, which entailed a global TN-RE of $51 \pm 3\%$. The reinoculation of MB-PBR contributed to maintaining the high share of TN removal but produced no significant increases in the performance of the photobioreactor compared to operation at a high HRT of 12.2 days (stage I).

Steady-state mass balance calculations revealed that assimilation was the main mechanism of nitrogen removal in PPB-PBR, accounting for 31, 27, 25 and 22% during stages I, II, III and IV, respectively. The enclosed configuration of the PPB-PBR contributed to low nitrogen stripping losses, with values of 16, 8, 16 and 16% in stages I, II, III and IV, respectively. However, the limited removal of nitrogen by PPB and their poor settleability contributed to a high loss of nitrogen in the PPB-PBR effluent (Table S3), with losses of 9–12% in the unsettled biomass and 53–65% in the form of dissolved nitrogen in the liquid effluent. The tolerance of PPBs to high ammonium concentrations allowed their application as a pretreatment for reducing nitrogen concentrations entering the sequential MB-PBR, thus avoiding inhibition of microalgae derived from high ammonia concentrations, as described in previous studies [41]. Mass-balances calculations in MB-PBR revealed that operation at a high HRT (12.2 days, stage I) resulted in a higher stripping ($\approx 43\%$) compared to stages II to IV operated at lower HRT (6.2 days), which showed lower shares of 9% (stage II), 12% (stage III) and 26% (stage IV). In this context, stripping of N_2 or NH_3 was likely the main mechanism of nitrogen removal in stages I and IV, also favoured by the slightly alkaline conditions and open configuration of MB-PBR. On the other hand, total assimilation in form of microalgal-bacterial biomass accounted for 29, 31, 27 and 21% of the nitrogen input in stages I, II, III and IV, respectively, representing the main removal mechanism in stages II and III.

3.2. Concentration and composition of biomass

Steady-state biomass concentrations in PPB-PBR (Fig. 4A) averaged $0.91 \pm 0.11 \text{ g TSS L}^{-1}$ in stage I, decreasing to 0.67 ± 0.07 and $0.72 \pm 0.07 \text{ g TSS L}^{-1}$ during stages II and III, respectively, mediated by the decrease in HRT. A slightly lower value of $0.57 \pm 0.08 \text{ g TSS L}^{-1}$ was recorded in stage IV. Overall, the concentration in PPB-PBR biomass remained very stable (mean value of $0.72 \pm 0.14 \text{ g L}^{-1}$ along all four stages), as confirmed by the measurement of the absorbance at 808 nm of cultivation broth (specific absorbance of bacteriochlorophyll α , characteristic of this type of microorganisms, Fig. S3). Previous studies of PWW treatment in PPB photobioreactors also reported a slight decrease in biomass concentration from 0.87 to 0.55 g L^{-1} when lowering the HRT from 10.6 to 4.1 days [4]. As reported by Hülsen et al. [38], the presence of biofilms attached to the photobioreactor walls might contribute to slight decreases in suspended PPB biomass concentrations in PPB photobioreactors. Indeed, photo-anaerobic membranes bioreactors can support higher PPB biomass concentrations in the range of $\approx 1\text{--}3.5 \text{ g L}^{-1}$ as a result of biomass retention [42] but at the expense of increasing the capital and operational costs associated with membrane operation. On the other hand, the small size of PPB entailed a low settleability, ultimately producing negative TSS-RE in the first settler in stages I to III, and low removal of only $14 \pm 8\%$ in stage IV (Fig. 3C). Future research is needed to cost-effectively enhance PPB biomass settleability. Implementing sequential batch operation may also favour biomass harvesting from culture broth [38]. The C, H, O, N and S content of PPB biomass averaged $51.7 \pm 1.2\%$, $7.6 \pm 0.2\%$, $22.4 \pm 1.2\%$, $8.2 \pm 0.5\%$ and $0.2 \pm 0.2\%$, respectively, which was similar to that previously reported for *R. palustris* ($55.1 \pm 0.2\%$, $8.5 \pm 0.0\%$, $28.1 \pm 0.2\%$ and $8.3 \pm 0.0\%$ for C, H, O and N, respectively) in an anaerobic photobioreactor fed with mineral medium and operated under semi-continuous mode [43].

Higher concentrations of biomass were recorded in MB-PBR compared to PPB-PBR. Thus, microalgae-bacteria biomass

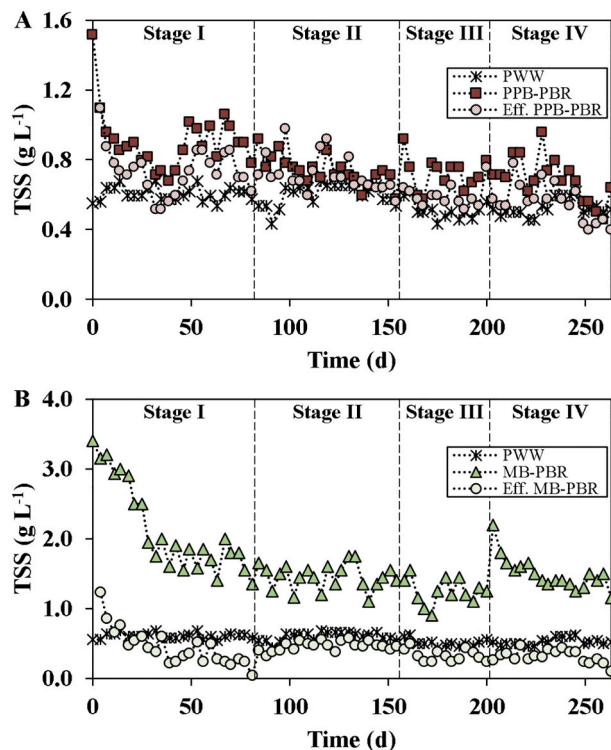


Fig. 4. Time course of the concentration of TSS in the influent PWW, cultivation broths and effluents of the PPB-PBR (A) and MB-PBR (B) during PWW treatment.

concentrations averaged 1.65 ± 0.26 , 1.37 ± 0.15 , 1.25 ± 0.12 and 1.35 ± 0.14 g TSS L⁻¹ in stages I, II, III and IV, respectively (Fig. 4B). The productivity of microalgae-bacteria biomass in MB-PBR was higher compared to that of PPB due to their efficient photoautotrophic metabolism and active CO₂ fixation [4,32]. Interestingly, the good settleability of the microalgae-bacteria biomass in the second settler supported TSS-REs of $101 \pm 14\%$, $47 \pm 7.7\%$, $70 \pm 23\%$ and $48 \pm 8.7\%$ in stages I, II, III and IV, respectively, which resulted in global TSS-RE of $76 \pm 10\%$, $40 \pm 4\%$, $51 \pm 12\%$ and $61 \pm 7\%$ during stages I, II, III and IV (Fig. 3C). Likewise, the C, H, O, N and S content of the microalgae-bacteria biomass averaged $50.7 \pm 2.7\%$, $7.5 \pm 0.1\%$, $25.0 \pm 2.8\%$, $8.6 \pm 0.3\%$ and $0.2 \pm 0.2\%$, respectively, which was very similar to the elemental composition of PPB biomass. The C:N ratio of the biomass harvested from both PPB-PBR and MB-PBR was approx. 5:1, thus suggesting a limitation of carbon for PPB and microalgae to assimilate all the nutrients present in PWW (exhibiting a C:N ratio of 2.5:1). In this sense, operational strategies aimed at increasing microalgae-bacteria biomass productivity may enhance nitrogen assimilation, but the carbon deficit may require the addition of an external carbon source such as CO₂.

PPB and microalgae biomass can be used as a feedstock to produce added value products [17,44]. Previous works have identified high concentrations of proteins, pigments (carotenoids and bacteriochlorophylls), pantothenic acid, coenzyme Q10 and biopolymers in PPB biomass [7,17], which could be derived during PWW treatment. Moreover, high concentrations of carbohydrates, lipids, proteins, pigments (carotenoids and chlorophylls) have been consistently reported in microalgae biomass [22]. In addition, the use of photosynthetic biomass as a food supplement in pig farming has been recently suggested due to its high content of protein, carbohydrates and essential oils, which would increase the sustainability of pig husbandry [28].

3.3. Microbial community analysis

3.3.1. Bacterial population

The analysis of sequencing of the gene 16S rRNA in PPB-PBR revealed that the inoculum of PPB was dominated by *Proteobacteria* at the phylum level. Overall, *Rhodopseudomonas* was the most abundant genus, with a relative abundance of 41% (Fig. 5), followed by *Dojka-bacteria* (10%), *Fastidiosipila* (10%) and *Proteiniphilum* (9%). *R. palustris*, *Rhodobacter sphaeroides* and *Rhodospirillum rubrum* are the most common purple non-sulfur bacteria found in wastewater treatment systems [7]. Some variations in the relative abundance of species in the PPB-PBR were observed along the four stages tested (Fig. 5). In stage I, *Rhodopseudomonas* was dominant, but its relative abundance declined to 24%.

Acinetobacter with a relative abundance of 9%, followed by *Fastidiosipila* (5%) and *Proteiniphilum* (4%), were also present at the end of stage I. This decrease in *Rhodopseudomonas* dominance was likely due to the adaptation of the inoculum to the operation under continuous PWW inflow. In addition, the decrease in HRT along with the washout of PPB biomass and the higher entrance of bacteria and archaea from the PWW during stage II resulted in the dominance of *Acinetobacter* (relative abundance 21%) followed by *Rhodopseudomonas* (18%). *Rhodopseudomonas* dominance was recovered during stages III and IV likely due to the increase in NIR radiation, which promoted a higher photosynthetic activity in PPB [13]. Indeed, *Rhodopseudomonas* exhibited relative abundances of 54% and 52% in PPB-PBR during stages III and IV, respectively.

Overall, purple non-sulfur bacteria are present in different types of wastewaters [17] under anaerobic conditions and sufficient NIR radiation [8,10]. *Rhodopseudomonas* has been identified in photobioreactors treating multiple types of wastewaters, with dominances of 30%, 60%, 74% and 82% during the treatment of agricultural [5], domestic [39], nitrogen-deficient wastewater [45] and piggery wastewaters [4], respectively. The dominance of PPB in these systems was mediated by the supply of sufficient NIR radiation and the maintenance of anaerobic conditions, which were previously described as the key factors favouring the growth of PPB over other heterotrophic bacteria [8,10]. In addition, a recent work reported that the supply of specific NIR radiation favoured a high dominance of PPB compared to other photosynthetic microorganisms (microalgae), which are inhibited under NIR radiation [38].

3.3.2. Microalgae population

The dominant microalgae species along the four operational stages was the chlorophyte *Mychonastes homosphaera* (Basionym: *Chlorella homosphaera*), which exhibited cell densities of 7.4×10^8 , 7.8×10^8 , 5.0×10^8 , 7.4×10^7 cell L⁻¹ in stages I, II, III, IV, respectively. These low concentrations of microalgae were likely due to the high concentration of suspended solids in the influent of the MB-PBR and the low concentration of inorganic carbon, which limited microalgae photosynthetic activity and growth during PWW treatment. *Mychonastes homosphaera* was detected under steady-state in all stages, with an abundance of 100% (Fig. S5) except in stage II, where *Tetrademus obliquus* was detected at a concentration of 3.0×10^7 cell L⁻¹ (4%). The main reason underlying *M. homosphaera* dominance was its high abundance in the inoculum (99% of the microalgae population) [19]. Even though the maintenance of microalgae monocultures is very difficult and rarely reported, a relatively high diversity of microalgae and bacteria communities dominates photobioreactors for wastewater treatment [20,31]. *M. homosphaera* seemed to be the microalgae species with higher

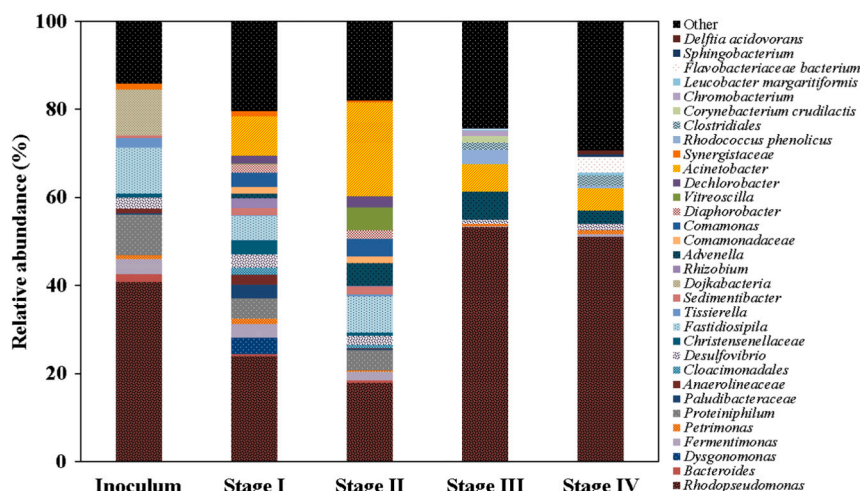


Fig. 5. Relative abundance (%) of the species in the PPB inoculum and cultivation broth of the PPB-PBR under steady-state in the four operational stages evaluated.

capacity to endure through time and dominate the MB-PBR, likely due to its tolerance to high ammonium and organic pollutant concentrations. *M. homosphaera* has been described as a promising workhorse for the treatment of wastewaters with high concentrations of emerging pollutants [46], and as a promising feedstock for animal feed supplements due to its high nutritional value in terms of its high content of protein, lipid and presence of metabolites with antioxidant capacity [47].

4. Conclusion

This study confirmed the potential of a novel configuration coupling a PPB-PBR to a MB-PBR for simultaneous carbon (up to 92%) and nitrogen removal (up to 86%). The efficient photoheterotrophic metabolism of PPB allowed high carbon assimilation, whereas microalgae-bacterial biomass enhanced nitrogen removal and the overall treatment performance due to its good settleability. High HRTs prevented biomass washout, whereas an increase in NIR radiation during operation at lower HRT enhanced photosynthetic activity in PPB, contributing to an overall enhancement of the PWW mediated treatment. The PPB-PBR was dominated mainly by *Rhodospseudomonas* sp., while the sequential MB-PBR configuration favoured the dominance of the microalga *M. homosphaera*. When combined, both photosynthetic microorganisms supported high assimilation of carbon and nitrogen in the form of biomass as the primary removal mechanism. Overall, PPB-PBR emerged as an effective pretreatment for microalgae-based treatment of PWW, thus demonstrating the high potential of combining PPB and microalgae during PWW treatment.

Declaration of competing interest

The authors declare no conflict of interest.

Acknowledgements

The financial support from the Regional Government of Castilla y León, the EU-FEDER programme (CLU 2017-09 and UIC 315) and CONICYT (PFCHA/DOCTORADO BECAS CHILE/2017 – 72180211) is gratefully acknowledged. The authors also thank Enrique Marcos, Araceli Crespo and Beatriz Muñoz for their technical assistance.

Appendix A. Supplementary data

Supplementary data to this article can be found online at <https://doi.org/10.1016/j.jwpe.2022.102825>.

References

- [1] G. Chen, J. Huang, X. Tian, Q. Chu, Y. Zhao, H. Zhao, Effects of influent loads on performance and microbial community dynamics of aerobic granular sludge treating piggery wastewater, *J. Chem. Technol. Biotechnol.* 93 (2018) 1443–1452, <https://doi.org/10.1002/jctb.5512>.
- [2] S.A. Lee, N. Lee, H.M. Oh, C.Y. Ahn, Stepwise treatment of undiluted raw piggery wastewater, using three microalgal species adapted to high ammonia, *Chemosphere* 263 (2021), 127934, <https://doi.org/10.1016/j.chemosphere.2020.127934>.
- [3] O. Yenigün, B. Demirel, Ammonia inhibition in anaerobic digestion: a review, *Process Biochem.* 48 (2013) 901–911, <https://doi.org/10.1016/j.procbio.2013.04.012>.
- [4] D. García, I. de Godos, C. Domínguez, S. Turiel, S. Bolado, R. Muñoz, A systematic comparison of the potential of microalgae-bacteria and purple phototrophic bacteria consortia for the treatment of piggery wastewater, *Bioresour. Technol.* 276 (2019) 18–27, <https://doi.org/10.1016/j.biortech.2018.12.095>.
- [5] T. Hülsen, K. Hsieh, Y. Lu, S. Tait, D.J. Batstone, Simultaneous treatment and single cell protein production from Agri-industrial wastewaters using purple phototrophic bacteria or microalgae – a comparison, *Bioresour. Technol.* 254 (2018) 214–223, <https://doi.org/10.1016/j.biortech.2018.01.032>.
- [6] D. Marín, E. Posadas, D. García, D. Puyol, R. Lebrero, R. Muñoz, Assessing the potential of purple phototrophic bacteria for the simultaneous treatment of piggery wastewater and upgrading of biogas, *Bioresour. Technol.* 281 (2019) 10–17, <https://doi.org/10.1016/j.biortech.2019.02.073>.
- [7] F. Capson-Tojo, D.J. Batstone, M. Grassino, S.E. Vlaeminck, D. Puyol, W. Verstraete, R. Kleerebezem, A. Oehmen, A. Ghimire, I. Pikaar, J.M. Lema, T. Hülsen, Purple phototrophic bacteria for resource recovery: challenges and opportunities, *Biotechnol. Adv.* 43 (2020), 107567, <https://doi.org/10.1016/j.biortechadv.2020.107567>.
- [8] F. Capson-Tojo, S. Lin, D.J. Batstone, T. Hülsen, Purple phototrophic bacteria are outcompeted by aerobic heterotrophs in the presence of oxygen, *Water Res.* 194 (2021), 116941, <https://doi.org/10.1016/j.watres.2021.116941>.
- [9] F.W. Larimer, P. Chain, L. Hauser, J. Lamerdin, S. Malfatti, L. Do, M.L. Land, D. A. Pelletier, J.T. Beatty, A.S. Lang, F.R. Tabita, J.L. Gibson, T.E. Hanson, C. Bobst, J.L.T.Y. Torres, C. Peres, F.H. Harrison, J. Gibson, C.S. Harwood, Complete genome sequence of the metabolically versatile photosynthetic bacterium *Rhodospseudomonas palustris*, *Nat. Biotechnol.* 22 (2004) 55–61, <https://doi.org/10.1038/nbt923>.
- [10] T. Hülsen, D.J. Batstone, J. Keller, Phototrophic bacteria for nutrient recovery from domestic wastewater, *Water Res.* 50 (2014) 18–26, <https://doi.org/10.1016/j.watres.2013.10.051>.
- [11] M. Stomp, J. Huisman, L.J. Stal, H.C.P. Matthijs, Colorful niches of phototrophic microorganisms shaped by vibrations of the water molecule, *ISME J.* 1 (2007) 271–282, <https://doi.org/10.1038/ismej.2007.59>.
- [12] C.N. Hunter, F. Daldal, M.C. Thurnauer, J.T. Beatty, *The Purple Phototrophic Bacteria, Advances in Photosynthesis and Respiration*, Springer Netherlands, Dordrecht, 2009.
- [13] C.A. Sepúlveda-Muñoz, I. de Godos, D. Puyol, R. Muñoz, A systematic optimization of piggery wastewater treatment with purple phototrophic bacteria, *Chemosphere* 253 (2020), 126621, <https://doi.org/10.1016/j.chemosphere.2020.126621>.
- [14] P. Dalaei, D. Ho, G. Nakhla, D. Santoro, Low temperature nutrient removal from municipal wastewater by purple phototrophic bacteria (PPB), *Bioresour. Technol.* 288 (2019), 121566, <https://doi.org/10.1016/j.biortech.2019.121566>.
- [15] T. Hülsen, E.M. Barry, Y. Lu, D. Puyol, D.J. Batstone, Low temperature treatment of domestic wastewater by purple phototrophic bacteria: performance, activity, and community, *Water Res.* 100 (2016) 537–545, <https://doi.org/10.1016/j.watres.2016.05.054>.
- [16] T. Hülsen, K. Hsieh, D.J. Batstone, Saline wastewater treatment with purple phototrophic bacteria, *Water Res.* 160 (2019) 259–267, <https://doi.org/10.1016/j.watres.2019.05.060>.
- [17] H. Lu, G. Zhang, Z. Zheng, F. Meng, T. Du, S. He, Bio-conversion of photosynthetic bacteria from non-toxic wastewater to realize wastewater treatment and bioresource recovery: a review, *Bioresour. Technol.* 278 (2019) 383–399, <https://doi.org/10.1016/j.biortech.2019.01.070>.
- [18] C.A. Sepúlveda-Muñoz, R. Ángeles, I. de Godos, R. Muñoz, Comparative evaluation of continuous piggery wastewater treatment in open and closed purple phototrophic bacteria-based photobioreactors, *J. Water Process Eng.* 38 (2020), 101608, <https://doi.org/10.1016/j.jwpe.2020.101608>.
- [19] D. Marín, A.A. Carmona-Martínez, S. Blanco, R. Lebrero, R. Muñoz, Innovative operational strategies in photosynthetic biogas upgrading in an outdoors pilot scale algal-bacterial photobioreactor, *Chemosphere* 264 (2021), 128470, <https://doi.org/10.1016/j.chemosphere.2020.128470>.
- [20] A.F. Torres-Franco, M. Zuluaga, D. Hernández-Roldán, D. Leroy-Freitas, C. A. Sepúlveda-Muñoz, S. Blanco, C.R. Mota, R. Muñoz, Assessment of the performance of an anoxic-aerobic microalgal-bacterial system treating digestate, *Chemosphere* 270 (2021), 129437, <https://doi.org/10.1016/j.chemosphere.2020.129437>.
- [21] APHA, *Standard Methods for the Examination of Water and Wastewater*, 21st ed., American Public Health Association, Washington, DC, USA, 2005.
- [22] R. Ángeles, E. Arnaiz, J. Gutiérrez, C.A. Sepúlveda-Muñoz, O. Fernández-Ramos, R. Muñoz, R. Lebrero, Optimization of photosynthetic biogas upgrading in closed photobioreactors combined with algal biomass production, *J. Water Process Eng.* 38 (2020), 101554, <https://doi.org/10.1016/j.jwpe.2020.101554>.
- [23] R. Schmieder, R. Edwards, Quality control and preprocessing of metagenomic datasets, *Bioinformatics* 27 (2011) 863–864, <https://doi.org/10.1093/bioinformatics/btr026>.
- [24] B.J. Callahan, P.J. McMurdie, M.J. Rosen, A.W. Han, A.J.A. Johnson, S.P. Holmes, DADA2: high-resolution sample inference from illumina amplicon data, *Nat. Methods* 13 (2016) 581–583, <https://doi.org/10.1038/nmeth.3869>.
- [25] C. Quast, E. Pruesse, P. Yilmaz, J. Gerken, T. Schweer, P. Yarza, J. Peplies, F. O. Glöckner, The SILVA ribosomal RNA gene database project: improved data processing and web-based tools, *Nucleic Acids Res.* 41 (2013) D590–D596, <https://doi.org/10.1093/nar/gks1219>.
- [26] J.G. Caporaso, J. Kuczynski, J. Stombaugh, K. Bittinger, F.D. Bushman, E. K. Costello, N. Fierer, A.G. Peña, J.K. Goodrich, J.L. Gordon, G.A. Huttley, S. T. Kelley, D. Knights, J.E. Koenig, R.E. Ley, C.A. Lozupone, D. McDonald, B. D. Muegge, M. Pirrung, J. Reeder, J.R. Sevinsky, P.J. Turnbaugh, W.A. Walters, J. Widmann, T. Yatsunenko, J. Zaneveld, R. Knight, QIIME allows analysis of high-throughput community sequencing data, *Nat. Methods* 7 (2010) 335–336, <https://doi.org/10.1038/nmeth.f.303>.
- [27] A. Sournia, *Phytoplankton Manual*, United Nations Educational, Scientific and Cultural Organization, Paris, 1978.
- [28] C.F. Silveira, L.R. de Assis, A.P. de S. Oliveira, M.L. Calijuri, Valorization of swine wastewater in a circular economy approach: effects of hydraulic retention time on microalgae cultivation, *Sci. Total Environ.* 789 (2021), 147861, <https://doi.org/10.1016/j.scitotenv.2021.147861>.
- [29] J.C. Fradinho, A. Oehmen, M.A.M. Reis, Photosynthetic mixed culture polyhydroxyalkanoate (PHA) production from individual and mixed volatile fatty acids (VFAs): substrate preferences and co-substrate uptake, *J. Biotechnol.* 185 (2014) 19–27, <https://doi.org/10.1016/j.jbiotec.2014.05.035>.
- [30] A. Navid, Y. Jiao, S.E. Wong, J. Pett-Ridge, System-level analysis of metabolic trade-offs during anaerobic photoheterotrophic growth in *Rhodospseudomonas*

- palustris*, BMC Bioinformatics 20 (2019) 233, <https://doi.org/10.1186/s12859-019-2844-z>.
- [31] T. Hülsen, K. Hsieh, S. Tait, E.M. Barry, D. Puyol, D.J. Batstone, White and infrared light continuous photobioreactors for resource recovery from poultry processing wastewater – a comparison, Water Res. 144 (2018) 665–676, <https://doi.org/10.1016/j.watres.2018.07.040>.
- [32] I. de Godos, S. Blanco, P.A. García-Encina, E. Becares, R. Muñoz, Long-term operation of high rate algal ponds for the bioremediation of piggery wastewaters at high loading rates, Bioresour. Technol. 100 (2009) 4332–4339, <https://doi.org/10.1016/j.biortech.2009.04.016>.
- [33] P. Bohutskyi, D.C. Kligerman, N. Byers, L.K. Nasr, C. Cua, S. Chow, C. Su, Y. Tang, M.J. Betenbaugh, E.J. Bouwer, Effects of inoculum size, light intensity, and dose of anaerobic digestion centrate on growth and productivity of *Chlorella* and *Scenedesmus* microalgae and their poly-culture in primary and secondary wastewater, Algal Res. 19 (2016) 278–290, <https://doi.org/10.1016/j.algal.2016.09.010>.
- [34] C. Chen, Y. Zhou, H. Fu, X. Xiong, S. Fang, H. Jiang, J. Wu, H. Yang, J. Gao, L. Huang, Expanded catalog of microbial genes and metagenome-assembled genomes from the pig gut microbiome, Nat. Commun. 12 (2021) 1–13, <https://doi.org/10.1038/s41467-021-21295-0>.
- [35] P. Dalaei, G. Bahreini, G. Nakhla, D. Santoro, D. Batstone, T. Hülsen, Municipal wastewater treatment by purple phototropic bacteria at low infrared irradiances using a photo-anaerobic membrane bioreactor, Water Res. 173 (2020), 115535, <https://doi.org/10.1016/j.watres.2020.115535>.
- [36] M.Y. Akhalaya, G.V. Maksimov, A.B. Rubin, J. Lademann, M.E. Darvin, Molecular action mechanisms of solar infrared radiation and heat on human skin, Ageing Res. Rev. 16 (2014) 1–11, <https://doi.org/10.1016/j.arr.2014.03.006>.
- [37] F. Vignola, J. Michalsky, T. Stoffel, Solar and Infrared Radiation Measurements, Second Edition, CRC Press LLC, 2019.
- [38] T. Hülsen, S. Stegman, D.J. Batstone, G. Capson-Tojo, Naturally illuminated photobioreactors for resource recovery from piggery and chicken-processing wastewaters utilising purple phototrophic bacteria, Water Res. 214 (2022), 118194, <https://doi.org/10.1016/j.watres.2022.118194>.
- [39] T. Hülsen, E.M. Barry, Y. Lu, D. Puyol, J. Keller, D.J. Batstone, Domestic wastewater treatment with purple phototrophic bacteria using a novel continuous photo anaerobic membrane bioreactor, Water Res. 100 (2016) 486–495, <https://doi.org/10.1016/J.WATRES.2016.04.061>.
- [40] O. Perez-Garcia, F.M.E. Escalante, L.E. De-Bashan, Y. Bashan, Heterotrophic cultures of microalgae: metabolism and potential products, Water Res. 45 (2011) 11–36, <https://doi.org/10.1016/j.watres.2010.08.037>.
- [41] I. de Godos, V.A. Vargas, S. Blanco, M.C.G. González, R. Soto, P.A. García-Encina, E. Becares, R. Muñoz, A comparative evaluation of microalgae for the degradation of piggery wastewater under photosynthetic oxygenation, Bioresour. Technol. 101 (2010) 5150–5158, <https://doi.org/10.1016/J.BIORTECH.2010.02.010>.
- [42] S. Chitapornpan, C. Chiemchaisri, W. Chiemchaisri, R. Honda, K. Yamamoto, Organic carbon recovery and photosynthetic bacteria population in an anaerobic membrane photo-bioreactor treating food processing wastewater, Bioresour. Technol. 141 (2013) 65–74, <https://doi.org/10.1016/j.biortech.2013.02.048>.
- [43] P. Carozzi, Hydrogen photoproduction by *Rhodospseudomonas palustris* 420L cultured at high irradiance under a semicontinuous regime, J. Biomed. Biotechnol. 2012 (2012) 1–8, <https://doi.org/10.1155/2012/590693>.
- [44] L. Christenson, R. Sims, Production and harvesting of microalgae for wastewater treatment, biofuels, and bioproducts, Biotechnol. Adv. 29 (2011) 686–702, <https://doi.org/10.1016/j.biotechadv.2011.05.015>.
- [45] I. de las Heras, R. Molina, Y. Segura, T. Hülsen, M.C. Molina, N. Gonzalez-Benítez, J.A. Meleró, A.F. Mohedano, F. Martínez, D. Puyol, Contamination of N-poor wastewater with emerging pollutants does not affect the performance of purple phototrophic bacteria and the subsequent resource recovery potential, J. Hazard. Mater. 385 (2020), 121617, <https://doi.org/10.1016/j.jhazmat.2019.121617>.
- [46] A. Rempel, G. Nadal Biolchi, A.C. Farezin Antunes, J.P. Gutkoski, H. Treichel, L. M. Colla, Cultivation of microalgae in media added of emergent pollutants and effect on growth, chemical composition, and use of biomass to enzymatic hydrolysis, Bioenergy Res. 14 (2021) 265–277, <https://doi.org/10.1007/s12155-020-10177-w>.
- [47] I. Saadaoui, M. Cherif, R. Rasheed, T. Bounnit, H. Al Jabri, S. Sayadi, R. Ben Hamadou, S.R. Manning, *Mychonastes homosphaera* (Chlorophyceae): a promising feedstock for high quality feed production in the arid environment, Algal Res. 51 (2020), 102021, <https://doi.org/10.1016/j.algal.2020.102021>.